Arabian Journal of Geosciences (2021) 14: 567
https://doi.org/10.1007/s12517-021-06947-1

ORIGINAL PAPER

Automatic detection of power transmission lines and risky object locations using UAV LiDAR data

Mustafa Dihkan[1] · Elif Mus[1]

Received: 5 March 2020 / Accepted: 11 March 2021 / Published online: 20 March 2021

Abstract

The periodic monitoring of energy lines to lessen the impacts of threats and to destroy the potential risks against the power transmission lines (PTL) is highly important. The risks can involve natural causes (vegetation, landslides, trees, avalanches, storms, etc.) on the one hand and the human factor (constructions and buildings breaking the safety distance, dumping the excavated material, theft, etc.) on the other hand. In this study, an algorithm, which can automatically detect PTLs' wires and pylons using the UAV LiDAR data, is developed. Specific safety distances are also spatially analyzed and the existence of risky ground objects is examined with the help of the detected PTLs. In the newly developed algorithm, ground points are located and the low object points in vertical distance to these ground points are eliminated using the cloth simulation filtering (CSF) method. The remaining point cloud is separated into voxels of 5×5×5m in size. In the search of 26 neighbor voxels, starting from automatically determined seed voxel, final detection of wire and pylons has been determined by the algorithm of "concave hull" after their straight slopes which are fitted by height values variant and RANSAC were analyzed. The accuracy value for wires was 97.13%, the integrity value was 97.36%, the quality value was 94.63%, for the pylons the accuracy value was 70.25%, the integrity value was 94.24% and the quality value was 67.36% in the algorithm developed. Periodic applications based on the proposed approach will make it easy to monitor and maintain PTLs components (wires and pylons) without time-consuming field works.

Keywords Power line · Pylon · LiDAR · Voxel · RANSAC

Introduction

Electrical energy has become very demanding in urban and industrial areas with its diversified usage capacity over the years. Therefore, important scientific research and innovation activities are carried out on electrical energy generation, transmission, and distribution systems (Ussyshkin et al. 2011). Especially in order to provide a fast and continuous energy supply, advanced energy distribution systems must be monitored with advanced technological methods with a high level of automation (Li and Guo 2018). In this way, the threats that can be caused by various factors (trees, buildings, corrosion, etc.) to power transmission lines (PTL) can be minimized and potential risks can be eliminated.

Today, thanks to the observation and automatic interpretation activities carried out by applying remote sensing technologies, the corrosion and mechanical deterioration of the PTL components (conductor wire, pylons, etc.) and the damages caused by storms and various natural disasters can be detected through simultaneous observation and analysis. In this way, serious economic losses can be prevented, and a high level of supply reliability can be ensured in advanced PTL systems. Besides, analysis of these data sets will prevent significant potential risks that may cause serious environmental problems such as forest fires and serious infrastructure damage due to various high objects (trees, buildings, etc.) located nearby the power lines (Matikainen et al. 2016).

Nowadays, LiDAR technology is used as another data source for semi-automatic or automatic detection of PTL components. Recent improvements in this remote sensing

Responsible Editor: Biswajeet Pradhan

✉ Mustafa Dihkan
mdihkan@ktu.edu.tr

Elif Mus
elffms@gmail.com

[1] Department of Geomatics, Faculty of Engineering, Karadeniz Technical University, 61080 Trabzon, Turkey

instrument over the last 10 years, the spatial density of point cloud data produced by airborne laser scanning (ALS) systems has been significantly increased and LiDAR sensors have been developed with the capability of recording data at different wavelength ranges of the electromagnetic spectrum. In addition, UAV LiDAR sensors are designed to be mounted on UAV platforms in parallel with the developments in UAV technology. By using UAV LiDAR sensors, point cloud data with very high horizontal/vertical spatial accuracy and areal density can be obtained in a short time with lower costs.

In this study, an algorithm has been developed to automatically detect some PTL components and various high objects that pose a risk to these components using UAV LiDAR data. By using the proposed approach, PTL components can be detected automatically without field surveys, so that the relevant control and inspection operations can be carried out quickly by saving from cost, time, and manpower. Therefore, the most important contribution of this study to the literature is that it enables full automatic detection of PTL components and risky objects in 3D space via point clouds produced by UAV LiDAR technology.

Related works

In recent years, various remote sensing techniques have been developed to monitor the components of the PTL and other land cover elements that may pose a potential risk to them (Pradhan and Sameen, 2020). In these approaches, a variety of remote sensing data sets such as multi-band optical imaging data, SAR (synthetic aperture radar) and thermal imaging data, ALS, or UAV LiDAR data have been utilized (Mu et al. 2009; Li et al. 2012). In the literature, machine learning-based approaches are also used to extract PTL components from LiDAR, optical, and other data sets. Generally, machine learning- or deep learning-based supervised classification methods (support vector machine, random forest, artificial neural networks, etc.) are implemented by using many user-defined parameters and training data sets (Wang et al. 2018; Abdollahi et al. 2020). User dependency resulting from the selection of a large number of parameters causes a significant decrease in the automation levels in these methods. Such dependencies, especially in high-density data sets such as LiDAR, result in high computational costs. In this section, various studies on PTL from past to present are generally summarized and presented.

Semi-automatic algorithms applied on aerial images have been developed for the detection of PTL cables in early literature studies (Li et al. 2010a). In these studies, Hough and Radon transforms are generally used for line detection in horizontal (XY) plane with the help of image processing techniques (Cheng et al. 2014; Liu et al. 2009; Li et al. 2010b; Grigillo et al. 2015).

Yan et al. (2007) proposed an algorithm, using the line detector mask over the optical image obtained from the line pixels in relation to the brightness, parallelism, and linearity by taking advantage of various geometric features that have identified the pixels belonging to the power line. However, after the segmentation of related pixel groups, Radon transformation was applied to each segment obtained. Thanks to this transformation, simultaneous line matching can be made for each segment by considering various features such as slope, start, and end distances. In the last stage, the Kalman filter was applied to fill missing adjacent line parts for these sections. However, Woods et al. (2004) used morphological filtering techniques and digital surface model (DSM) generated from InSAR data to detect vertical objects. With this approach, PTL components were determined using criteria based on height, size, and shape. Yan et al. (2012) used the X band SAR images produced by TerraSAR and COSMO-Skymed satellites to reveal the relationship between the visibility on the SAR image and the backscatter values of the power line components (pylon and conductor wires). Also, Sha et al. (2014) examined the backscattering behavior of the six-conductor power line segment using a time series of 20 TerraSAR images (Matikainen et al. 2016).

With the developments in LiDAR technology, the number of studies on the detection of PTL components using LiDAR point cloud data is increasing in the literature. Jwa and Sohn (2012) proposed the reconstruction method called piecewise model growing (PMG) and used the 2D line equation for two different geometric forms to estimate the orientation of the transmission lines based on the catenary model with hyperbolic cosine function in the XZ plane. Axelsson (1999) has classified parallel power lines in the 2D XY plane by applying the Hough transformation model. In order to shorten the search time and increase the algorithm performance, it is suggested that the search process where the parallel lines of the power line are compared with different object edges which do not have any direction information, is made using the corridor area limitation.

Because of the complexity of the LiDAR data compared to optical data, it is important to identify and classify the points of the energy cables in the first stage in order to gradually reduce the data density in algorithms designed for semi-automatic or automatic detection of PTL components such as power cables, pylons, and connectors (Sohn et al. 2012). The PTL components can be located close to the buildings in urban areas and high objects such as vegetation in rural areas. This problem reduces the detection accuracy and speed of the approaches that provide solutions for the automatic detection problem (Wang et al. 2017). Therefore, in order to classify the points of the energy line from the general data in some proposed approaches, it is tried to estimate the curve parameters of the line by using the fragmented curvature properties of the

line. For this purpose, Sohn et al. (2012) used the PMG technique. In the first stage of PMG, LiDAR point cloud data is divided into voxels of appropriate size considering the distance between the lines. Then, the energy line was determined by using various properties of points in neighboring voxels such as linearity, clustering (closeness), density, and continuity (catenary) in the same direction. Melzer and Briese (2004) using the Hough transform for parallel line detection in the XY plane by dividing the line into sub-sections and applying curve fitting techniques to each section. In a similar approach, Jwa et al. (2009) applied Hough transformation using eigenvectors and point density, and a fragmented catenary curve model growth algorithm was developed to identify points in each power line. McLaughlin (2006) tried to predict iterative catenary parameters starting from an arbitrary local affine model by calculating the local affine parameters of the transmission lines in each ellipsoidal neighborhood with the proposed algorithm. Finally, the power line was modeled through the collection of all local affine models. Chan and Lichti (2011) showed that catenary curves with different directions and shapes can be modeled effectively in 3D space with the help of the models defined by using the parameters such as distance, rotation, translation, and scaling of the points on the curve to the gravity center. In addition, it has been stated that this approach can also be used for the self-calibration of mobile LiDAR systems. Zhang et al. (2016) proposed an approach capable of detecting power lines based on the direction of expansion with the seed-based region growing technique. With this algorithm, a railway power line can be separated quickly and automatically from the complex rail system. Guo et al. (2016) proposed a RANSAC-based method using contextual pylon information and the distribution of the wire group between two neighboring pylons to improve power line reconstruction results. The main assumption here is that the power lines in a group have a parallel geometry and close sag values in the same direction, and that this information can be effectively used to estimate the initial parameters required to construct the 3D PTL model. Although several approaches have been proposed for the solution of the automatic detection problem of PTL components in various studies, desired accuracy rates and automation levels have not been achieved in different studies yet. For this reason, researches to minimize detection errors caused by buildings and vegetation close to power lines and to increase detection accuracy are continuing intensively (Chen 2007).

Awrangjeb (2019) proposed the power line corridors (PLC), pylons, and wires detection approach. In this approach, PLCs are extracted from the point cloud data, and each PLC consists of a set of rectangular regions that connect serially with each other. Then, only points within each rectangular PLC region are considered to locate and extract pylons. The non-ground points between two successive pylons of the same PLC are used to extract individual wires. Munir et al. (2020) proposed an automated method for extracting individual sub-conductors in bundles from the complex structure of PLCs using the combination of image and point-based approaches.

On the other hand, it is very important to observe and detect various man-made or naturally occurring objects (buildings, vegetation, etc.) in the PTL corridors (Matikainen et al. 2016). Algorithms developed for automatic observation and detection of such objects using ALS or UAV LiDAR data aim to predict potential risks to PTL components. Besides, the relevant automatic monitoring and detection approaches allow the detection of damaged parts in the PTL components for different reasons and subsequent maintenance of these parts in a short time (Kim and Sohn 2010).

Materials and methods

In this study, a region of 136.06 hectares with the semi-urban land cover character was selected as a study area in Priceville, AL, USA. Point cloud data was generated by scanning PTL components and other land cover elements in the study area with a Velodyne HDL-32 UAV LiDAR sensor using a 905-nm wavelength laser beam. The point cloud data obtained after the scanning process have 17 points/m^2 areal density and ±2 cm spatial accuracy. The data set was referenced in UTM projection (Fig. 1).

In this study, an algorithm has been developed that can automatically detect PTL components and various high objects that create risks to them by using UAV LiDAR data. In the first stage of the algorithm, ground and above-ground points were determined, and in the following stage, low points near the ground were eliminated; then voxelization was performed and various distinctive features were extracted for each voxel, and after that, the wire and pylon points were separated by applying the voxel neighborhood-based segmentation process; and in the last stage, risky object points were determined. The flowchart of the algorithm is shown in Fig. 2. After applying the proposed algorithm to the test data set in Matlab environment, wire and pylon points from PTL components and various high object points that create a risk to them are automatically classified.

Determination of ground and above-ground points

In the literature, several semi-automatic and automatic filtering algorithms have been developed to detect the ground points from LiDAR point cloud data (Wan et al. 2018). These algorithms can yield different accuracy levels depending on many parameters such as land topographic structure, land cover, urban, semi-urban or rural land use characteristics of the region, and point density of LiDAR point cloud data (Briese 2010). With such algorithms, more successful results can be obtained in areas with low slope topography and low

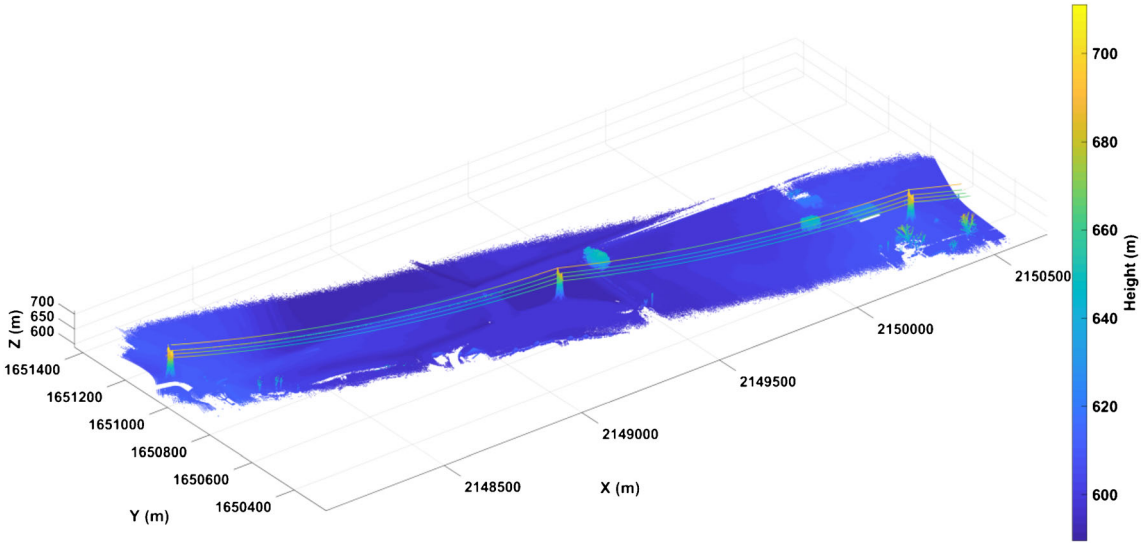

Fig. 1 Study area

above-ground object density. On the other hand, the detection accuracy of the ground points may decrease in regions with high slope topography and having various variable-sized above-ground objects (buildings, vegetation, poles, power lines, etc.) (Meng et al. 2010). In the first stage of the proposed approach, the ground points were automatically detected by using the cloth simulation filtering (CSF) algorithm, which was minimally affected by such conditions. The CSF algorithm is an algorithm that can automatically classify the point cloud as ground and non-ground using five parameters (fabric thickness representing the simulated field surface topography, grid resolution expressing the horizontal distance between two adjacent particles, ground and non-ground points classification threshold, time threshold controlling the displacement of particles due to gravity, and simulation iteration value), depending on the distance between the raw point cloud and a simulated land surface with a fabric cover in mind (Zhang et al. 2016). After applying this algorithm to the sample data set, the classified ground and non-ground points are depicted in Fig. 3.

Elimination of low points near the ground

In the second stage of the proposed approach, a triangular surface model was created according to the "Delaunay triangulation" method using the ground points identified in the previous stage in order to eliminate the low points near the ground. At this stage, 3D distances from low points close to the ground to triangular surfaces were calculated using the KNN (k-nearest neighbor) algorithm. The 20-m distance threshold was then applied to eliminate the points of the low objects, and only the points of the high objects and the power line were kept in the data (Fig. 4).

Voxelization and voxel feature determination

At this stage of the study, ground points were eliminated and the point cloud was divided into voxels representing certain standard sub-volumetric regions in 3D space. In this way, various geometry, shape, texture, etc. features can be derived for each voxel point cloud. In the study, 6067 voxels were formed in 5×5×5m dimensions and related indices and center of gravity were determined for each of them. Then, the height values variance was calculated for the point cloud within each voxel. In addition, by using RANSAC, inlier points, and related slope, intercept parameters showing the most appropriate distribution with line model at 0.5 m search distance in XY plane were calculated and recorded for each voxel.

Automatic filtering according to height values variance

At this stage, an automatic threshold value (t) was determined by a histogram-based Otsu thresholding algorithm using height variance values calculated for each voxel. Then, the voxels with a variance value greater than $t/10$ were eliminated. In this way, some of the points belonging to high objects other than power lines are also filtered (Fig. 5).

The Otsu thresholding algorithm is a histogram-based approach and is a widely used automatic threshold value detection method on gray-level images. Based on the assumption that the data consists of two classes, the object of interest and other objects, the algorithm can determine the threshold value over the features. For this purpose, in-class and inter-class variance values are used in the algorithm. For all threshold values, the in-class variance value of these two classes is calculated by Eq. (1).

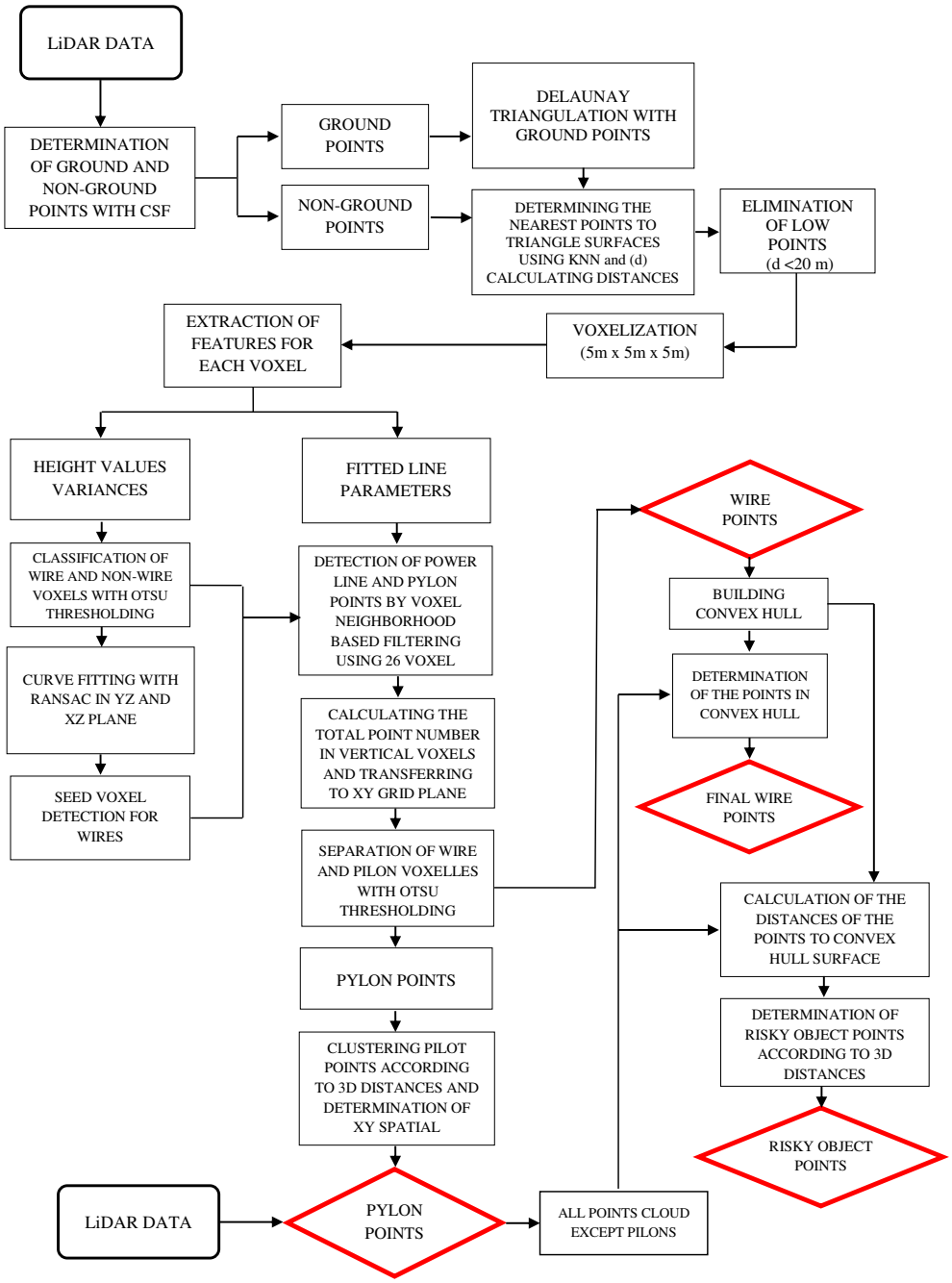

Fig. 2 Flow chart

$$\partial^2 = \sum_{i=1}^{N} (x - x_i)^2 \Pr(x_i) \quad (1)$$

In the equation, x_i is the weighted average, and $Pr\ (x_i)$ is the probability function. The threshold value that ensures the minimum variance is considered the optimum threshold value. In this case, while the in-class variance value is at minimum, the inter-class variance value is at maximum. Because the calculation of variance value between classes requires fewer operations, it is possible to get faster results by calculating variance between background and foreground classes (Otsu 1979).

Seed voxel determination

When considered globally, it is a known prior geometric condition that all points forming power lines show the linear distribution in the XY plane and curvilinear distribution in the XZ and YZ planes. From this point of view, all remaining points after filtering according to the height variance were analyzed with RANSAC, and among these points, inlier points that were in linear distribution in the XY plane and in the 2nd order curvilinear distribution in YZ and XZ planes were determined. In addition, the index values of voxels that

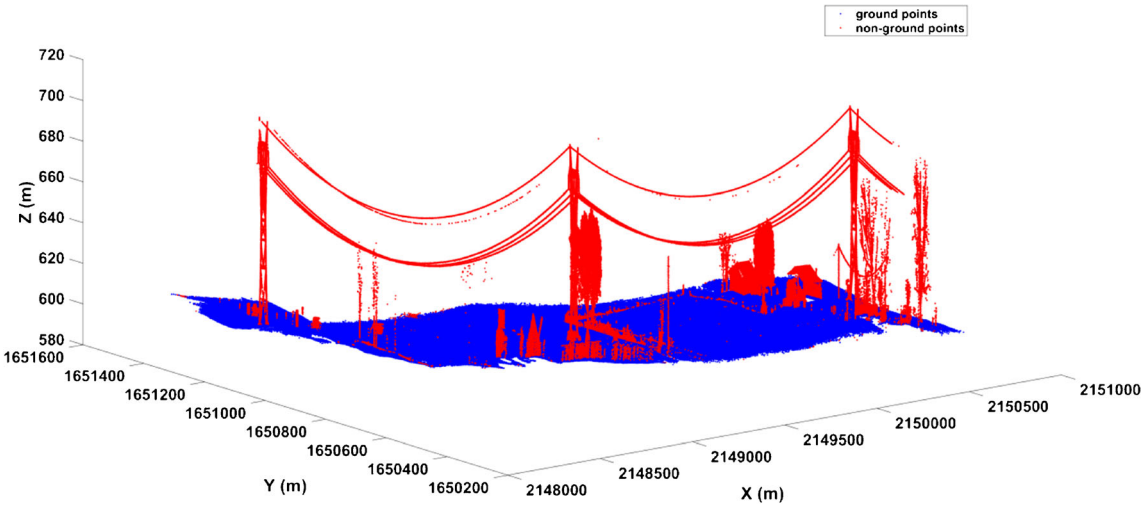

Fig. 3 Classified ground (colored blue) and non-ground points (colored red)

contain these inlier points were determined and recorded simultaneously. These voxels certainly contain power line points, of which one was randomly selected as seed voxel. The voxels detected at this stage include only a portion of the wire and pylon points identified in the final decision stage of the algorithm, which is used for seed voxel detection only (Fig. 6a).

Detection of power line and Pylon points by voxel neighborhood-based filtering

In the proposed algorithm, in order to filter the points of other high objects other than wires and pylons, the 3D distances of the voxel center of gravity positions were determined from the automatically determined seed voxel in the previous stage and the nearest 26 neighbor voxels were determined and the feature relations between them were examined. In the iterative search process starting from the automatically determined seed voxel, the voxels with the absolute slope difference less than 5, one of the previously determined line parameters for the center and the nearest 26 candidate voxels, were assigned as wire and pylon voxel (Fig. 6b). The search was continued until all voxels were finished and the points of the wires and pylons were determined (Fig. 6c).

Separation of power line and pylon points

At this stage of the algorithm, the separation of the determined wire and pylon points from each other and the recovery of the incorrectly classified points belonging to the wire or pylon in the previous filtering processes were performed. For this purpose, previously determined wire and pylon voxels were represented in the 2D XY grid plane. As a further step, the total number of points in all vertical voxels in each grid area is

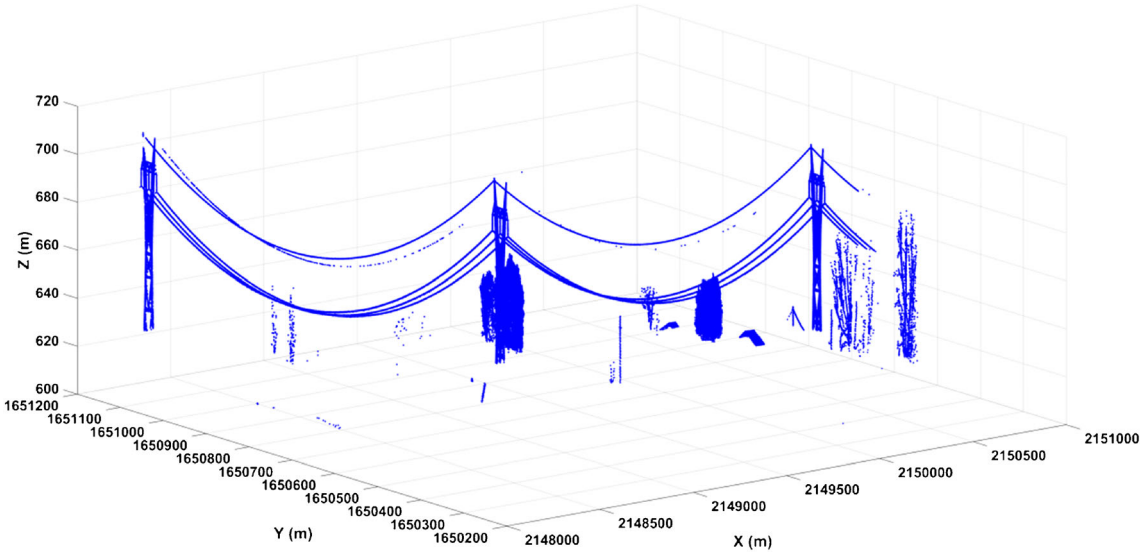

Fig. 4 High object points

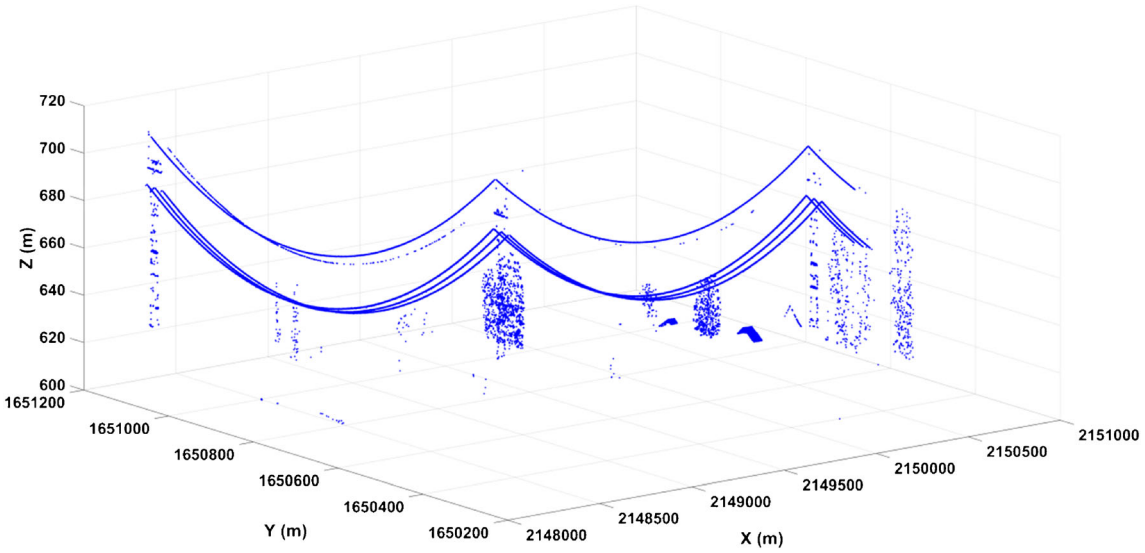

Fig. 5 Points filtered by height values variance

calculated and assigned as the corresponding grid value in the XY plane. In this way, a significant difference appears between pylon grid values and wire grid values in the XY plane. Otsu's automatic threshold value was calculated from the histogram generated by the grid point numbers. By using this threshold value, wire and pylon voxels and the points within these voxels were separated and classified. Although all pylon voxels have been detected at this stage because there is more than one pylon, the points in these voxels should be spatially clustered and boundaries of these clusters should be determined. For this purpose, a clustering process was carried out based on the 3D distances of the pylon points to each other. Finally, the clustering process was completed by using the prior knowledge that the 3D distance between the two pylons should be more than a certain value. In this process, the corner coordinates (x, y) that define each pylon area in the XY plane were obtained. In this way, the points at all heights within the boundaries determined by the (x, y) coordinates from all unfiltered LiDAR data were labeled as pylon points (Fig. 7). Then all the remaining points were separated and saved as wire points.

In order to recover the small number of points that were eliminated during the previous wire points detection steps, a concave hull was created using the determined points to define the volume of the points (Fig. 8).

Then, all points remaining inside the concave hull volume from unfiltered point cloud data (pylon points removed) were detected by spatial analysis to obtain the final wire points (Fig. 9a).

Risky object analysis with concave hull

In the final stage of the proposed approach, various risky object points closer to conductor wires than certain 3D distances are automatically detected. For this purpose, the 3D distances of the high points to the concave hull surface produced in the previous stage were calculated with the KNN algorithm. The obtained distances were evaluated and risky object points were determined in two different categories as 0-20 m and 20-30m. The concave hull, wire, and risky object points can be seen in Fig. 10.

Results

In the proposed algorithm, the wire and pylon points automatically detected from the whole point cloud were labeled and recorded. The wire and pylon points extracted by the proposed algorithm can be seen in Fig. 9.

For the accuracy analysis, correctness (*Corr*), completeness (*Comp*), and quality (Q) accuracy metrics, widely accepted in the literature, have been utilized to present the performance of the algorithm with quantitative data and compare it with other algorithms (Rutzinger et al. 2009; Jwa and Sohn 2012). The accuracy metrics can be calculated from the reference data with Eqs. (2), (3), and (4), respectively.

$$Corr = \frac{(TP)}{(TP) + (FP)} \tag{2}$$

$$Comp = \frac{(TP)}{(TP) + (FN)} \tag{3}$$

$$Q = \frac{(TP)}{(TP) + (FN) + (FP)} \tag{4}$$

In the equations, *Corr* is the correct matching ratio, *Comp* is the automatic detection level, Q is the quality percentage of the application, *TP* is the number of matching points with reference data determined by the proposed algorithm, *FN* is the number of detail points in the reference

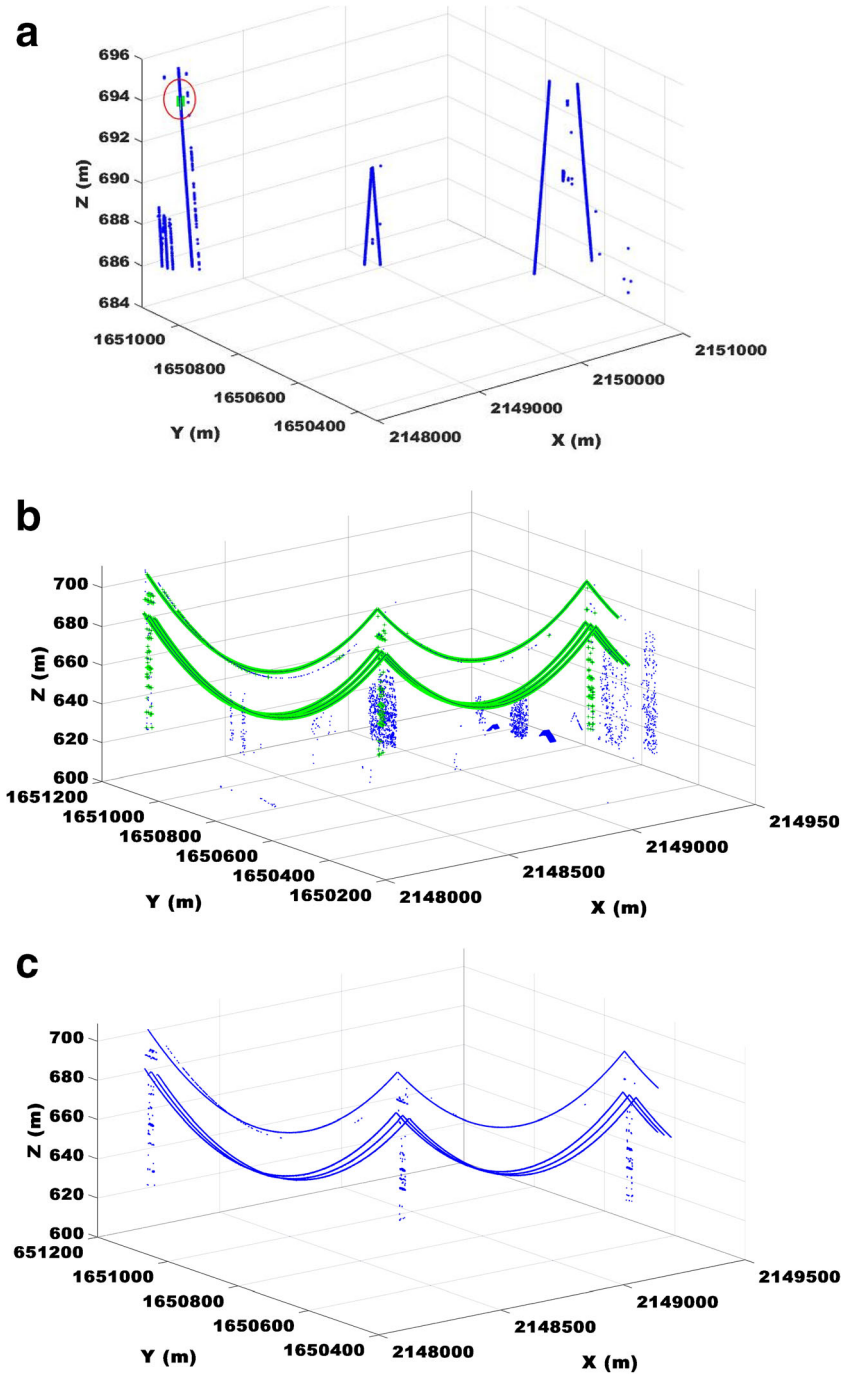

Fig. 6 (a) Seed voxel detection (b) Filter by voxel neighborhood (Green Points) (c) Power Line and Pylon points after filtering according to voxel neighborhoods

data that cannot be detected by the algorithm, and *FP* refers to the number of detail points detected by the algorithm but not in the reference data.

A reference data set was produced by manually classifying and labeling the test data as wire and pylon points for the accuracy analysis. After the automatic classification of wire and pylon objects by the proposed algorithm, accuracy metrics were calculated using the result and reference data sets (Table 1).

In the last stage of the study, the process of determining risky object points that may pose a danger to PTL components

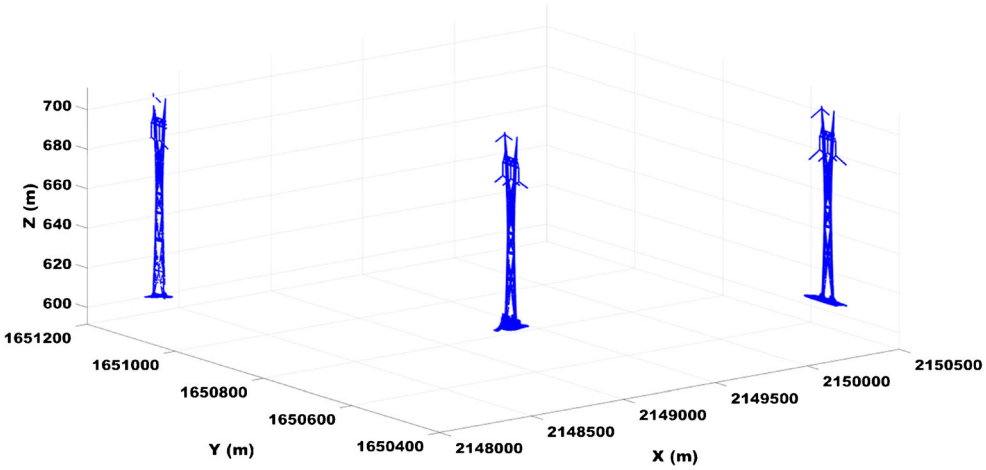

Fig. 7 Pylons detected by the proposed algorithm

and classifying them according to the risk status was automatically performed. The concave hull created for this purpose and classified risky object points are shown in Fig. 10.

Discussion

The performance of the proposed algorithm calculated by the accuracy metrics has been compared quantitatively with various algorithms available in the literature. At this stage, it was observed that 8 of the 10 power line sections were completely detected and 2 of them were partially detected. This is because the point density in the respective wire sections is quite low. Most of the similar studies in the literature have been carried out only for the detection of PTL wires. In some of these studies, accuracy evaluation was made based on only the correctness metric, while in others, both correctness and completeness criteria were taken into account (Table 2). When Table 1 is examined, as a result of subjecting the PTL wires automatically detected with the proposed approach to the accuracy analysis together with the reference data set, it is understood that the correctness (precision) value is 97.13%, and the completeness (recall) value is 97.36%.

The accuracy values obtained by using various semi-automatic or automatic algorithms developed for power line detection in the literature are presented in Table 2.

When the proposed algorithm is compared with other algorithms using accuracy metrics stated in Tables 1 and 2, it is understood that the proposed algorithm has the same or higher performance level as the other algorithms. However, while ALS-based LiDAR data were used in most of the studies, UAV LiDAR data was used by few studies. The high density of point clouds in UAV LiDAR data compared to classical ALS systems positively affects the detection accuracy of PTL components. On the other hand, the geometrical features that can change instantaneously due to external factors such as wind and vibration can reduce the performance of the approaches that include the fitting process to the catenary model. Chen et al. (2018), which is a similar study in that it uses a UAV LiDAR data set, obtained 96.50% and 94.80% correctness and completeness values, respectively, using an iterative fitting-based approach to the Euclidean distance-based clustering and catenary curve model. However, in order to minimize the effects caused by the aforementioned anomalies, clearance anomaly detection was performed. The proposed approach in this study has been tried to use a minimum number of parameters, and histogram-based automatic threshold

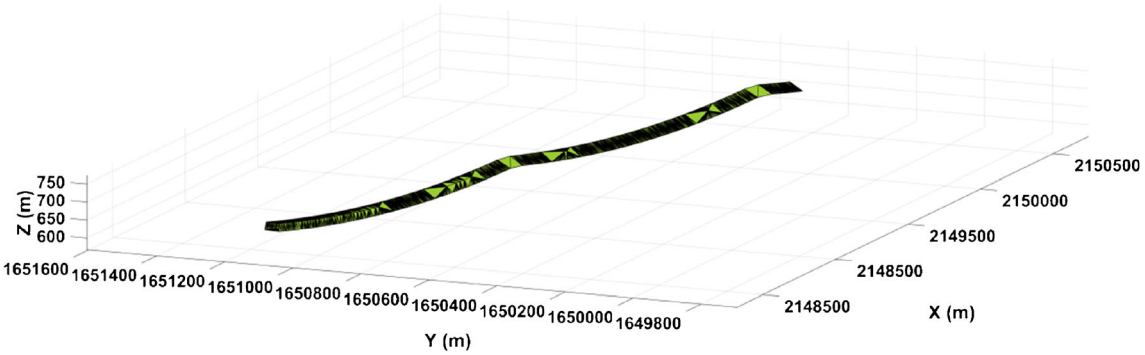

Fig. 8 Concave hull created with wire points

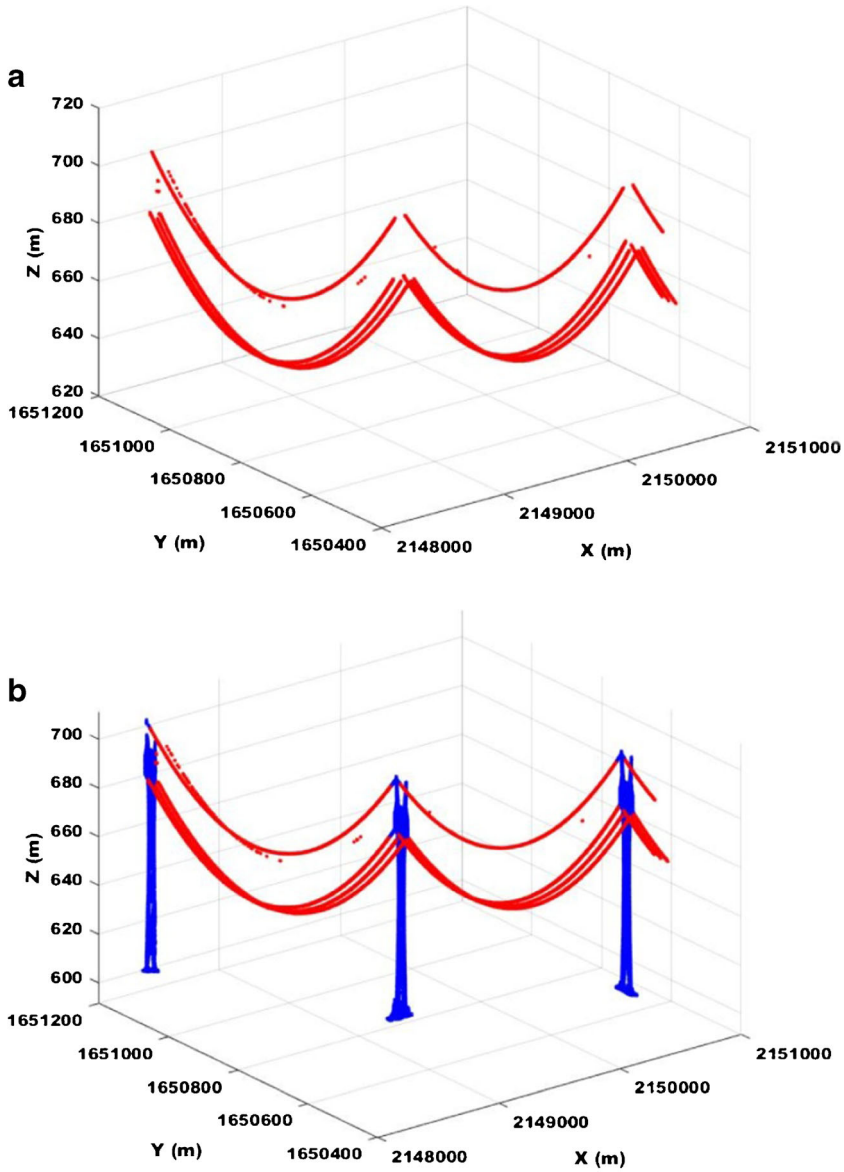

Fig. 9 **a** Detected wire points. **b** Combination of wire (red-colored) and pylon points (blue colored)

values have been used in the thresholding stages. In addition, the RANSAC method was used in the curve fitting processes, which can provide high fitting performance even with very few inlier sample data. In this way, the negative effects of the variations that may occur in the geometric features are minimized. Accordingly, similar results were obtained in the study with Chen et al. (2018). Munir et al. (2020) proposed an approach for fully automatic detection of individual conductors in PTL components. This approach has categorized horizontal and vertical objects with distance-based neighborhood analysis by using geometric features produced after voxelization. In this way, the approach reached 98.1% correctness and 97.2% completeness values in determining individual conductors for PTL components. On the other hand, in the approach proposed by Munir et al. (2020), a large number of fixed distance threshold values between the parameters used were defined and used to directly affect the decision processes. This situation reveals the possibility of a decrease in the approach performance in determining the PTL components with different geometric characteristics in rural areas with dense trees with different land topography. Yermo et al. (2019) reached 99.24% and 94.50% correctness and completeness values, respectively, by using the iterative candidate search and then hough transformation for the catenary model in the approach proposed for fully automatic detection of PTL components. However, it is seen that erroneous determination during the iterative candidate search stage negatively affects the performance of the algorithm, especially in areas with dense vegetation. As a result of this, it has been revealed that the completeness value decreases. Kim and Sohn (2013), Guo et al. (2016), and Wang et al. (2017a, b) tried to detect PTL components and other land cover elements using supervised

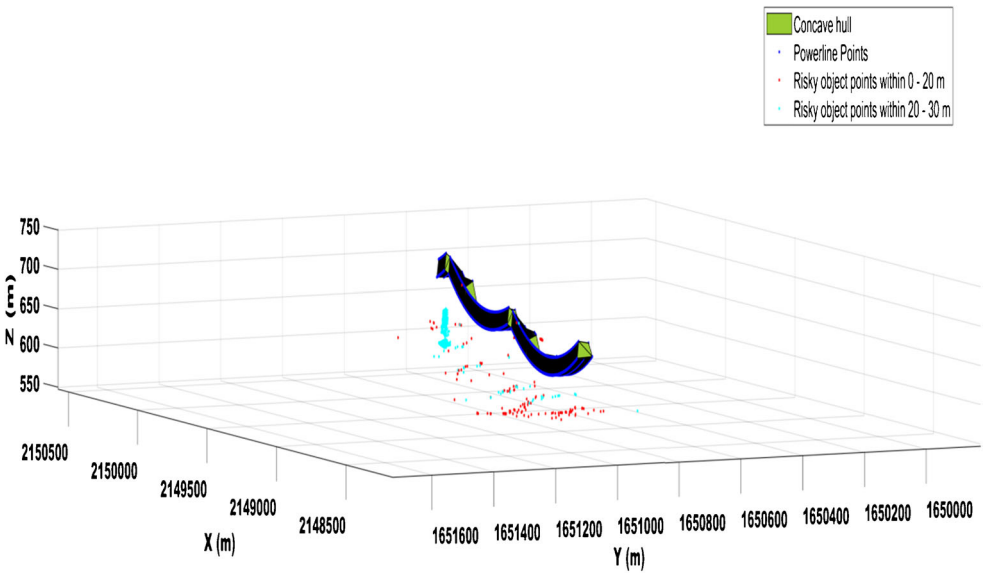

Fig. 10 Concave hull, wire, and risky object points

or semi-supervised algorithms such as random forest, joint boost, and support vector machine. In these approaches, it is understood that sufficient accuracy levels cannot be reached despite user dependency and low automation levels.

Conclusion

In recent years, electrical energy has become more essential for humanity than ever before. In fact, highly cost-effective PTL components are installed and operated with labor-intensive procedures in order to deliver electrical energy from the places where it is produced or stored to consumption points. Today, especially in developed urban areas, even in case of instant cuts in electricity supply may cause high-cost problems. This situation can also cause serious problems in terms of living comfort and safety. Therefore, in order to ensure a high level of energy supply reliability, (1) it is very important to detect the damage caused by natural or human causes in PTL components in a short time to minimize the effect, and (2) continuous monitoring is essential to eliminate the potential risks to PTL components. Nowadays, remote sensing techniques are used to perform such observation and detection activities with high spatial accuracy, in a short time, and with minimum human intervention. In this study, an algorithm that automatically detects power lines, pylons, and various high object positions that may pose risk to these PTL components is developed by using UAV LiDAR data which is one of the advanced remote sensing instruments. In the algorithm, an approach is proposed that can gradually reduce the high density and complexity of LiDAR data, including PTL components and other land cover objects. At different stages of the algorithm, the descriptive local and global features of the data were extracted using voxel structure and RANSAC optimization techniques to be used in decision-making processes. Therefore, approximately 97% detection accuracy has been achieved with the proposed algorithm. As a result, periodic monitoring of PTL elements using UAV LiDAR technology and the proposed algorithm will allow all kinds of inspection and maintenance procedures to be performed on the lines without the need for field surveys. UAV LiDAR technology is very sensitive to environmental factors such as wind and vibration besides its low cost, high

Table 1 Accuracy metrics for power line and pylon objects

Classes	Correctness (%)	Completeness (%)	Quality (%)
Power line	97.13	97.36	94.63
Pylon	70.25	94.24	67.36

Table 2 Power line detection results for different algorithms

Algorithms	Correctness (%)	Completeness (%)
Munir et al. (2020)	98.10	97.20
Awrangjeb (2019)	98.10	97.20
Yermo et al. (2019)	99.24	94.50
Chen et al. (2018)	96.50	94.80
Bhola et al. (2018)	88.13	77.99
Wang et al. (2017a, b)	98.44	83.06
Yadav and Chousalkar (2017)	98.80	90.80
Guo et al. (2016)	89.00	86.00
Zhu and Hyyppä (2014)	93.26	-
Cheng et al. (2014)	93.90	-
Kim and Sohn (2013)	93.08	-
McLaughlin (2006)	86.90	-

automation level, and sensitive surface representation. Although the proposed approach is minimally affected by these impacts due to its nature, improvements can be made to provide robustness against this weakness in order to achieve higher performance in the future. Higher accuracy levels can be achieved by making use of the spectral-based information to be obtained by UAV LiDAR sensors, which can simultaneously receive data at different wavelengths of the electromagnetic spectrum, especially in order to minimize errors caused by high vegetation. In the future, it is thought that the proposed algorithm can produce more successful results in accordance with advancements in UAV LiDAR sensor technology that can offer high spatial point density and better spectral resolution.

Acknowledgements The authors are grateful to Fagerman Technologies, dba, LiDARUSA for providing the UAV LiDAR data.

References

Abdollahi A, Pradhan B, Shukla N, Chakraborty S, Alamri A (2020) Deep learning approaches applied to remote sensing datasets for road extraction: a state-of-the-art review. Remote Sens 12(9):1444

Axelsson P (1999) Processing of laser scanner data, algorithms and applications. ISPRS J Photogramm 54(2-3):138–147

Awrangjeb M (2019) Extraction of power line pylons and wires using airborne LiDAR data at different height levels. Remote Sens 11(15): 1798

Pradhan B, Sameen MI (2020) Laser scanning systems in highway and safety assessment. Springer, Berlin/Heidelberg

Bhola R, Krishna NH, Ramesh KN, Senthilnath J, Anand G (2018) Detection of the power lines in UAV remote sensed images using spectral-spatial methods. J Environ Manage 206:1233–1242

Briese C (2010) Extraction of digital terrain models. In: Vosselman G, Maas H G, Air borne and Terrestrial Laser Scanning. CRC Press Boca Raton: 147-150

Chan T, Lichti DD (2011) 3D catenary curve fitting for geometric calibration. Int Arch Photogramm 38:259–264

Chen Q (2007) Airborne LiDAR data processing and information extraction. Photogramm Eng Rem S 73:109–112

Chen C, Yang B, Song S, Peng X, Huang R (2018) Automatic clearance anomaly detection for transmission line corridors utilizing UAV-Borne LIDAR data. Remote Sens 10:613

Cheng L, Tong L, Wang Y, Li M (2014) Extraction of urban power lines from vehicle-borne LiDAR data. Remote Sens 6:3302–3320

Grigillo D, Ozvaldič S, Vrečko A, Fras MK (2015) Extraction of power lines from airborne and terrestrial laser scanning data using the Hough transform. Geodetski Vestnik 59:246–261

Guo B, Li Q, Huang X, Wang C (2016) An improved method for power-line reconstruction from point cloud data. Remote Sens 8(1):36

Jwa Y, Sohn G, Kim HB (2009) Automatic 3D power line reconstruction using airborne LiDAR data. Int Arch Photogramm 38:105–110

Jwa Y, Sohn G (2012) A piece-wise catenary curve model growing for 3D powerline reconstruction. Photogramm Eng Rem S 78(12): 1227–1240

Kim HB, Sohn G (2010) 3D classification of power-line scene from airborne laser scanning data using random forests. Int Arch Photogramm 38(3A):126–132

Kim HB, Sohn G (2013) Point-based classification of power line corridor scene using random forests. Photogramm Eng Rem S 79(9):821–833

Li WH, Tajbakhsh A, Rathbone C, Vashishtha Y (2010a) Image processing to automate condition assessment of overhead line components. In: Proc. 2010 1st International Conference on Applied Robotics for the Power Industry (CARPI), IEEE, October, Montreal

Li X, Guo Y (2018) Application of LiDAR technology in power line inspection. In: IOP Conference Series: Materials Science and Engineering 382(5), IOP Publishing

Li Z, Liu Y, Walker R, Hayward R, Zhang J (2010b) Towards automatic power line detection for a UAV surveillance system using pulse coupled neural filter and an improved Hough transform. Mach Vis Appl 21(5):677–686

Li Z, Bruggemann TS, Ford JJ, Mejias L, Liu Y (2012) Toward automated power line corridor monitoring using advanced aircraft control and multisource feature fusion. J Field Robot 29(1):4–24

Liu Y, Li Z, Hayward R, Walker R, Jin H (2009) Classification of airborne LiDAR intensity data using statistic analysis and Hough transform with application to power line corridors. In: Proceedings of the Digital Image Computing: Techniques and Applications Conference, December, Melbourne, Australia, pp 462-467

Matikainen L, Lehtomäki M, Ahokas E, Hyyppä J, Karjalainen M, Jaakkola A, Kukkoand A, Heinonen T (2016) Remote sensing methods for power line corridor surveys. ISPRS J Photogramm 119:10–31

McLaughlin RA (2006) Extracting transmission lines from airborne LiDAR data. IEEE Geosci Remote S 3(2):222–226

Meng X, Currit N, Zhao K (2010) Ground filtering algorithms for airborne LiDAR data: a review of critical issues. Remote Sens 2:833–860

Melzer T, Briese C (2004) Extraction and modeling of power lines from ALS point clouds. In: Proc. of 28 Workshop of Austrian Association for Pattern Recognition, Hangenberg, Austria, pp 47-54

Mu C, Yan Q, Feng Y, Caiand J, Yu J (2009) Overview of power lines extraction and surveillance using remote sensing technology. In: MIPPR 2009: Remote Sensing and GIS Data Processing and Other Applications (Vol. 7498, p. 74981M). International Society for Optics and Photonics

Munir N, Awrangjeb M, Stantic B (2020) Automatic extraction of high-voltage bundle subconductors using airborne LiDAR data. Remote Sens 12(18):3078

Otsu N (1979) A Threshold Selection Method from Gray-Level Histograms. IEEE T Syst Man Cyb 9(1):62–66

Rutzinger M, Rottensteiner F, Pfeifer N (2009) A comparison of evaluation techniques for building extraction from airborne laser scanning. IEEE J Sel Top Appl 2(1):11–20

Sha L, Tao L, Mingzhou W, Ailing H, Wenhao W, Kan X, Yan L (2014) Study on extra-high voltage power line scatterers in time series SAR. In: 2014 Third International Workshop on Earth Observation and Remote Sensing Applications (EORSA) IEEE, pp 47-51

Sohn G, Jwa Y, Kim HB (2012) Automatic powerline scene classification and reconstruction using airborne LiDAR data. In: ISPRS Annals of Photogrammetry, Remote Sensing and Spatial Information Sciences 13(167172):28

Ussyshkin RV, Theriault L, Sitar M, Kou T (2011) Advantages of airborne lidar technology in power line asset management. In Proceedings of the 2011 International Workshop on Multi-Platform/Multi-Sensor Remote Sensing and Mapping (M2RSM), Xiamen, China, pp 1-5

Wan P, Zhang W, Skidmore AK, Qi J, Jin X, Yan G, Wang T (2018) A simple terrain relief index for tuning slope-related parameters of LiDAR ground filtering algorithms. ISPRS J Photogramm 143: 181–190

Wang Y, Chen Q, Liu L, Zheng D, Li C, Li K (2017b) Supervised classification of power lines from airborne LiDAR data in urban areas. Remote Sens 9:771

Wang Y, Chen Q, Li K, Zheng D, Fang J (2017a) Airborne LIDAR power line classification based on spatial topological structure characteristics. In: ISPRS Annals of Photogrammetry, Remote Sensing and Spatial Information Sciences (Vol. 4)

Wang Y, Chen Q, Liu L, Li X, Sangaiah AK, Li K (2018) Systematic comparison of power line classification methods from ALS and MLS point cloud data. Remote Sens 10(8):1222

Woods D, Folley C, Kwan YT, Houshmand B (2004) Automatic extraction of vertical obstruction information from interferometric SAR elevation data. In: Proc. IEEE International Geoscience and Remote Sensing Symposium (IGARSS'04) 6:3938–3941

Yadav M, Chousalkar CG (2017) Extraction of power lines using mobile LiDAR data of roadway environment. Remote Sens Appl Soc Environ 8:258–265

Yan L, Ailing H, Sha L, Xingkai L, Wenhao W, Tao L (2012) High voltage power line scattering feature analysis in multi SAR sensors and dual polarization. In: Proc. 2012 Second International Workshop on Earth Observation and Remote Sensing Applications (EORSA), IEEE, June, Shanghai, China, pp 225–229

Yan G, Li C, Zhou G, Zhang W, Li X (2007) Automatic extraction of power lines from aerial images. IEEE Geosci Remote S 4(3):387–391

Yermo M, Martínez J, Lorenzo OG, Vilarino DL, Cabaleiro JC, Pena TF, Rivera FF (2019) Automatic detection and characterisation of power lines and their surroundings using LiDAR data. Int Arch Photogramm 4213:1161–1168

Zhang W, Qi J, Wan P, Wang H, Xie D, Wang X, Yan G (2016) An easy-to-use airborne LiDAR data filtering method based on cloth simulation. Remote Sens 8(6):501

Zhu L, Hyyppä J (2014) Fully-automated power line extraction from airborne laser scanning point clouds in forest areas. Remote Sens 6(11):11267–11282